UCRL-TR-155814

LAWRENCE
LIVERMORE
NATIONAL
LABORATORY

Limits to enhanced IR layering set by long scale ablator roughness

Bernard J. Kozioziemski.

December 12, 2003

DISCLAIMER

This work was performed under the auspices of the U. S. Department of Energy by University of California, Lawrence Livermore National Laboratory under Contract W-7405-Eng-48.

Target Area Technologies Program

Mail Station L - 472

Ext: 4-6317

December 12, 2003

MEMORANDUM

TO: Distribution

FROM: Bernard Kozioziemski

SUBJECT: Limits to enhanced IR layering set by long scale ablator roughness.

I. SUMMARY

We show that long scale-length ablator roughness sets a limit to the enhanced IR layering power possible in a NIF ignition hohlraum. This limit can be more restrictive than the limit set by thermal conduction. High IR power absorption, characteristic of the ablator material, combined with ablator roughness can produce ice thickness variations which exceed the NIF ice layer roughness specification. For example, if the capsule IR absorption coefficient is greater than 13 cm^{-1}, the max IR power is less than the 4 Q_{DT} limit set by thermal conduction.

II. INTRODUCTION

Infrared heating of hydrogen ice layers inside of plastic capsules is a demonstrated method to decrease the ice surface roughness. As with native beta-layering, the ice surface tends to conform to an isotherm when heated by IR. Infrared absorption in the ablator far exceeds the absorption in D-T[1]. Thus, asymmetries in the capsule lead to asymmetries in the innermost ice isotherm which causes distortions in the inner ice surface. IR heating of the ice layer mitigates the effect of asymmetries in the capsule, but this mitigation is less effective when the ratio of capsule to ice heating is large. Since the ice redistributes to follow an isotherm, the ice layer is impacted by temperature variations due to thickness variations in the capsule.

NIF specifications for both the ice and ablator uniformity[2] show that ablator roughness is required to be much less than ice layer roughness in current designs. For modes 2-4, the allowed ablator thickness variation is 75 nm, compared to 400 nm for the ice layer. This memo studies the relation between capsule and ice thickness variations when infrared heating is used. Limits to IR heating are determined based on the NIF ablator specification.

III. CALCULATION

A simple 1-D approximation is used for calculation of the ice layer thickness perturbation δi as a function of capsule thickness differences δc given specific capsule and ice bulk heating rates. The 1-D geometry is a good approximation for long scale-length modes since it does not take into account heat flow transverse to the surface. Transverse heat flow will tend to reduce temperature differences inside the capsule, thus this calculation sets an upper limit on δi for a given δc. The calculation is similar to previous treatments[3], but includes capsule heating as well as ice heating.

The outer capsule is in thermal contact with the exchange gas at T_0 as shown in Fig. 1. The capsule has thickness c_1 on the left and c_2 on the right, with $\delta c = c_2 - c_1$. Identical bulk heating rates Q_c are used in both sides of the capsule. Similar definitions apply to the D-T ice layer with a bulk heating rate of Q_i. The heat flux across the D-T ice–vapor interface is set to

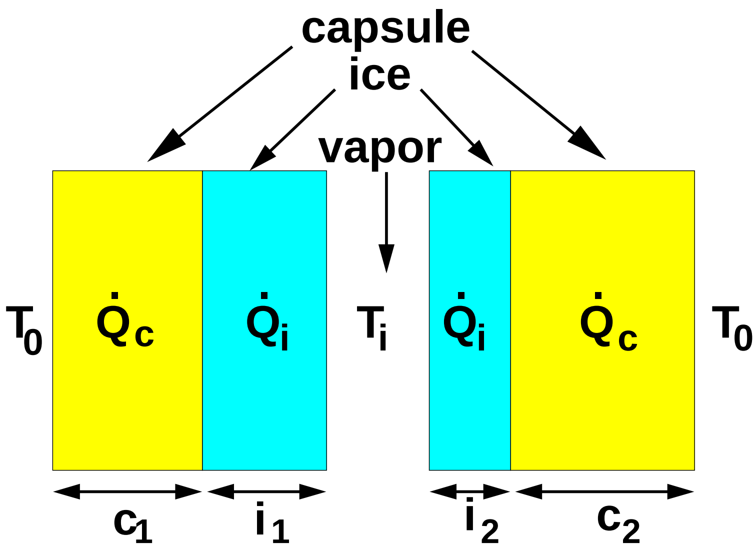

FIG. 1: Geometry used to solve the 1D problem. A layer of ice is on each side of the capsule, with no heat conduction between the two sides in steady state. The outer capsule surfaces are kept at T_0. Q_c and Q_i are the bulk heating rates in the capsule and ice, respectively. At equilibrium, the inner ice surfaces will be at the same temperature T_i. Given a thickness difference in the capsule (δc = c_2-c_1), the ice thickness difference (δi = i_2-i_1) is solved with specified Q_c and Q_i.

zero.

The 1D temperature field in each region is given by

$$T_j(x) = -\frac{1}{2}\frac{Q_j}{k_j}x^2 + A_j x + B_j, \tag{1}$$

where j is either the capsule (c) or the ice (i), Q_j is the bulk heating rate in region j, k_j is the thermal conductivity, and A_j and B_j are integration constants. The four boundary conditions on the left are

$$T(x = 0) = 0,$$

$$\frac{\partial T_i}{\partial x}|_{(c_1+i_1)} = 0,$$

$$T_i(x = c_1) = T_c(x = c_1),$$

$$k_i \frac{\partial T_i}{\partial x}|_{c_1} = k_c \frac{\partial T_c}{\partial x}|_{c_1}, \tag{2}$$

with identical expressions for the right side. Solving for the temperature at the inner ice surface gives

$$T_i(c_1 + i_1) = \frac{1}{2}\frac{Q_c}{k_c} c_1^2 + \frac{1}{2}\frac{Q_i}{k_i} i_1^2 + c_1 i_1 \frac{Q_i}{k_c}. \tag{3}$$

A similar result is found for the right side. We require that the inner ice temperatures be identical on both sides and use $c_2 = c_1 + \delta c$ and $i_2 = i_1 + \delta i$. Then solving for δi gives a quadratic equation for δi

$$(\delta i)^2 \left(\frac{1}{2}\frac{Q_i}{k_i}\right) + \delta i \left(\frac{Q_i}{k_i} i_1 + \delta c \frac{Q_i}{k_c} + c_1 \frac{Q_i}{k_c}\right) + \frac{Q_c}{k_i}\left(c_1 \delta c + \frac{1}{2}(\delta c)^2\right) + \frac{Q_i}{k_c} i_1 \delta c = 0. \tag{4}$$

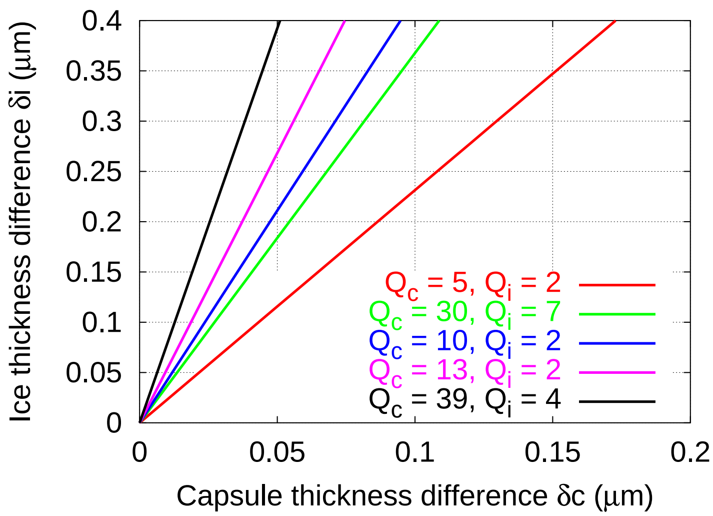

FIG. 2: Ice thickness difference resulting from a capsule thickness difference for several different Q_c and Q_i values. The ice thickness difference δi is nearly linear in the capsule thickness difference δc over the range shown. The calculations assumed a 2 mm diameter NIF capsule with 150 μm thick ablator and 80 μm thick ice layer.

The ice perturbation δi can be obtained exactly from Eqn. 4 and thus serves to illustrate key features of the problem. Formulating the problem in a hohlraum geometry does not lead to significant changes in the resulting thickness perturbation. However, the solution in the hohlraum geometry provides more stringent constraints on the capsule roughness. The difference between the two models is that the outer capsule surface is held at constant temperature in the first case, while the hohlraum wall is the fixed temperature in the hohlraum geometry. The hohlraum model was used to generate the figures. Equation 4 still serves to illustrate key features of the problem.

Figure 2 show a plot of δi for a given δc and various heating rates. The parameters used are k_i = 0.3 W/(m·K)[4], k_c = 0.175 W/(m·K)[5], Q_{DT} = 50000 W/m^3, i_1 = 80.0 μm, c_1 = 150.0 μm. The values of Q_c and Q_i are given in multiples of Q_{DT}. The ice heating, Q_i, contains 1 Q_{DT} of native beta-layering, with the remainder from IR heating. A capsule absorption coefficient α_c = 10.0 cm^{-1} is used in the cases shown by the curves with Q_c = 5 and Q_c = 30. Q_c = 5 has 1 Q_{DT} of beta-layering and 1 Q_{DT} from the IR in the ice; Q_c = 30 is the maximum amount of IR heating possible for this capsule that can be conducted through the hohlraum. A capsule absorption of α_c = 23.0 cm^{-1} is used in the cases shown for Q_c = 13 and Q_c = 39. These two cases show 1 Q_{DT} of IR into the ice and the maximum ice IR heating, respectively.

The nearly linear dependence of δi on δc is due to the similar thermal conductivities and thicknesses of the ice and capsule. It is helpful to approximate Eqn. 4 as

$$\delta i \approx \frac{-\delta c\left(\frac{Q_c}{Q_i}\frac{k_c}{k_i}c_1 + i_1\right)}{c_1 + \frac{k_c}{k_i}i_1}. \tag{5}$$

The ratio Q_c/Q_i is 0.07-20 for absorption coefficients considered. As Q_c goes to zero, $\delta i = 0.4\delta c$ using the same thermal conductivities and capsule geometry as above. However, for Q_c/Q_i greater than 0.8, δi is larger than δc.

The ice perturbations due to capsule asymmetries are calculated assuming that the capsule is at the specification for wall uniformity. The discussion is restricted to the first few

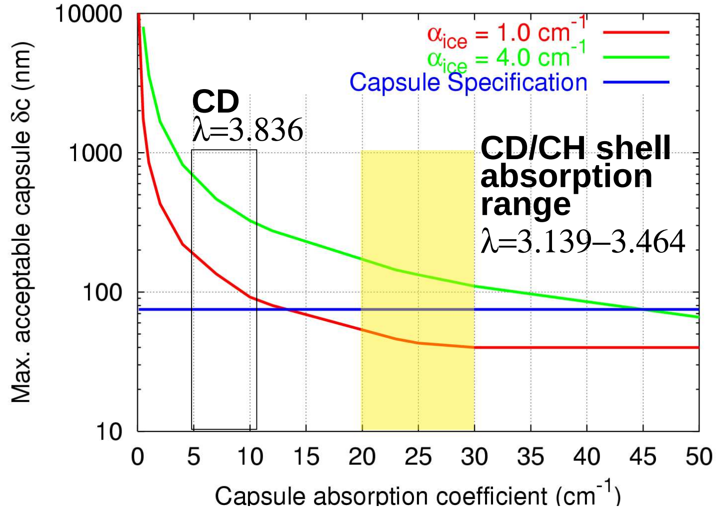

FIG. 3: Maximum tolerable capsule thickness difference δc for the ice δi not to exceed the 400 nm specification as a function of capsule absorption coefficient α_c. Cases for the ice absorption coefficient of 1.0 cm^{-1} and 4.0 cm^{-1} are shown. The IR power was chosen as the maximum in the thermal conduction limit and 1 $Q_{\rm DT}$ from native beta-layering was included.

modes because of the 1D approximation. NIF specification for the ablator thickness difference at long scale-lengths is 75 nm and the ice thickness difference must be less than 400 nm. Figure 3 shows the maximum tolerable capsule thickness difference as a function of the capsule absorption coefficient for two different ice absorption coefficients. The low mode capsule specification of 75 nm is shown as well. The maximum IR power that can be conducted from the capsule through the hohlraum assembly to the NIF cryostat was used for each α_c[6]. For δc greater than 75 nm, the IR heating is limited by thermal conduction, while for δc less than 75 nm, the IR heating is limited by the capsule specification. The case for D_2, where α_i is 4.0 cm^{-1} is much more tolerable to ablator roughness than the D-T case of 1.0 cm^{-1}. The D_2 case is limited by the thermal conduction in all but the highest α_c cases. The IR heating for D-T is limited by the capsule smoothness specification for $\alpha_c > 13$ cm^{-1}.

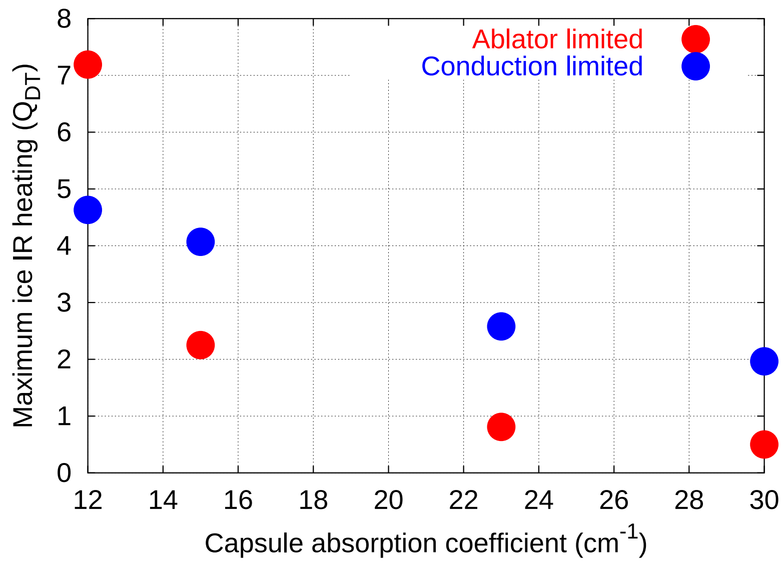

FIG. 4: Maximum possible IR heating of the ice layer inside a hohlraum as a function of capsule absorption coefficient α_c. The ablator limited points assume ablator 75 nm wall thickness perturbations are allowed to grow to 400 nm in the ice layer with α_i = 1.0 cm^{-1} and unlimited heat conduction. The conduction limited points assume the IR is limited only by the conduction of heat to the NIF cryostat. The IR heating limit is reduced by a factor of 2-4 when the ablator roughness is included compared to the conduction only limit for α_c larger than 15 cm^{-1}.

Figure 4 shows the maximum IR heating for a few different α_c when the capsule thickness variations are 75 nm and α_i = 1.0 cm^{-1}. There is a rapid decrease in $Q_{\rm DT}$ heating of the ice as α_c increases. Below α_c of 12 cm^{-1}, the IR heating is unlimited by δ_x of 75 nm. This is evident from Eqn. 5. Using the ratio of δi to δc of 400/75 = 5.3, the NIF capsule dimensions of $c_1 \approx 2i_1$, and k_c/k_i = 0.58, then

$$\begin{aligned} \frac{Q_c}{Q_i} &= 1.48\frac{\delta i}{\delta c}, \\ &= 7.8. \end{aligned} \tag{6}$$

Including 1 $Q_{\rm DT}$ from beta-heating, this ratio is obtained for α_c = 14.7 cm^{-1}.

The calculations so far have assumed that α_i is 1.0 cm^{-1} for D-T ice. A higher value of α_i = 2.0 cm^{-1} would double the acceptable α_c to 19 cm^{-1} at which the IR is limited by the ablator roughness rather than thermal conduction. The current CD and CH capsules have $\alpha_c \approx$ 21-29 for wavelengths where the D-T absorption may have the higher value of 2 cm^{-1}[7]. Should a future measurement confirm that α_i = 2.0 cm^{-1} for D-T then long scale-length capsule roughness should not adversely affect IR layering.

IV. CONCLUSION

We have shown that IR heating of a D_2 layer is not limited by the ablator roughness for values of the capsule absorption coefficient consistent with CH, CD and deuterated polyimide capsules when these capsules meet the NIF wall thickness specification. However, for D-T, with a lower α_i = 1.0 cm^{-1}, the value of α_c needs to be less than 10 - 12 cm^{-1} to prevent capsule perturbations from imprinting on the ice layer. A larger α_c requires either a reduced IR heating or a smoother ablator.

---

[1] R. C. Cook, A. Nikroo, S. A. Letts, *LLNL memo, Measurement of Wavelength Dependent Extinction Coefficients for Target Capsule Materials*, Livermore, **2001**.

[2] S. W. Haan, T. Dittrich, G. Strobel, S. Hatchett, D. Hinkel, M. Marinak, D. Munro, O. Jones, S. Pollaine, and L. Sutter, “Update on Ignition Target Fabrication Specifications”, *Fusion Science and Technology*,**41**, pp. 164–173 (2002).

[3] A. J. Martin, R. J. Simms, R. B. Jacobs, ”Beta Energy Driven Uniform Deuterium-Tritium Ice Layer in Reactor-Size Cryogenic Inertial Fusion Targets”, *J. Vac. Sci. Technol. A*, **6**, pp. 1885-1888 (1988).

[4] G. W. Collins, P. C. Souers, E. M. Fearon, E. R. Mapoles, R. T. Tsugawa, J. R. Gaines, "Thermal Conductivity of Condensed D-T and T_2", *Phys. Rev. B.*,**41**, pp. 1816-1823 (1990).

[5] J. D. Moody, R. A. London, J. J. Sanchez, "Experimental and Theoretical Characterization of the Actively Controlled Thermal Environment in a Cryogenic Hohlraum", *Fusion Science and Technology*, **45** pp. 27-32 (2004).

[6] B. J. Kozioziemski, *LLNL memo, Re-Assessing the maximum allowed infrared (IR) power for enhanced layering in a conduction dominated cryogenic NIF-scale hohlraum.*, Livermore, **2003**.

[7] R. C. Cook, A. Nikroo, *LLNL memo, IR Extinction Coefficient Measurement of CH and CD GDP Shells*, Livermore, **2003**.